Analysis of the Behavior of Digital Protections of Transmission Lines When Subjected to Frequencies Outside the Operating Range, in a Real Case

Giovanni B. Fabris, Claudenei S. Simão and Marcelo L. Poleto

Analysis of the Behavior of Digital Protections of Transmission Lines When Subjected to Frequencies Outside the Operating Range, in a Real Case

Giovanni B. Fabris [iD]*†, Claudenei S. Simão [iD]†, Marcelo L. Poleto [iD]†

Eletrobras CGT Eletrosul†

Email: gfabris@eletrobras.com*

Abstract—**This paper reports on the improper operation of the overvoltage protection, in a real case, due to the estimation error of its phasors, when the frequency of the voltage signal was not compatible with the sampling frequency. It was possible to observe the recovery time of the frequency tracking signal. The results obtained by applying the simulation of the occurrence in the IED are also illustrated, as well as an analysis of the concepts applied in the calculations of the IED phasors. Thus, the conclusion is presented by exposing the solution adopted for the referred problem.**

Keywords—**Overvoltage protection, Phasor estimation, Frequency tracking, Incorrect protection performance**

I. Introduction

Correct estimation of the voltage and current phasors of the terminals of a transmission line (LT) is necessary for Intelligent Electronic Devices (IEDs) algorithms to be able to perform their protection and control functions properly. Phasor estimation algorithms [1][2][3] typically use a sliding window, the size of which is determined by the number of samples used in this window [1], and defined as a function of the nominal frequency or the estimated frequency of the power system [4]. Frequency tracking (FT) algorithms, such as zero crossing [5], can be used to find the frequency of the power system at a given time by measuring the voltage and current signals [6][7]. Therefore, determining the actual frequency of the network signals is of utmost importance, since their phasors are directly related to this frequency.

To determine voltage phasors, IED manufacturers use several strategies, such as a Half-Cycle Fourier Filter (HCFF) [8], which can be associated with pre-filtering to reject distortions from Capacitive Voltage

Transformers [9], as well as a One-Cycle Fourier Filter (OCFF) [10][11].

This paper presents a real case in which the incorrect operation of the overvoltage function occurred due to a failure in the phasor estimation, caused by the delay in determining the correct system frequency. It was found that the frequency tracking algorithm used by the IED of the transmission line under study requires a certain amount of time to stabilize. The solution obtained by analyzing this case promoted adjustment procedures in protection IEDs, where the choice of the correct analog channel to be the frequency reference for the frequency tracking algorithm is determined.

This paper is structured as follows. Section 2 describes the disturbance and presents the problem of incorrect operation of the overvoltage function due to a failure in the phasor estimation. Section 3 presents the laboratory tests, through fault simulations. Section 4 describes some frequency tracking techniques. Section 5 discusses some phasor estimation algorithms. Section 6 compares the algorithms with the real case. Section 7 presents the solution to the problem. And, in Section 8, the main conclusions are shown.

II. Description of the Disturbance

The 230 kV LT shutdown was caused by a single-phase short circuit (phase C to ground). The instantaneous protections operated correctly and the automatic reclosing was successful at both terminals. The simplified single-line diagram of the line is illustrated in Fig. 1.

During the dead time of the automatic reclosing, the line voltage measured, at both terminals, oscillates at a frequency between 45Hz and 46Hz, due to the energy exchange between the shunt reactor and the line
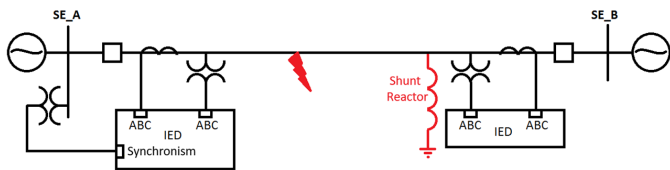
Figure 1: Simplified diagram of the 230 kV LT

capacitances. Approximately 480 ms after the line was reclosed, at the SE-A terminal, the first to close, the overvoltage protection incorrectly operated, causing the three-pole circuit breaker at this terminal to open.

The oscillography of the IED protection at the SE-A terminal, with the voltage and current waveforms, is detailed in Fig. 2, where it can be seen that the voltage, after automatic reclosing, was close to its pre-fault value, in the order of 1.0 pu, and there were no conditions for the overvoltage protection to operate.
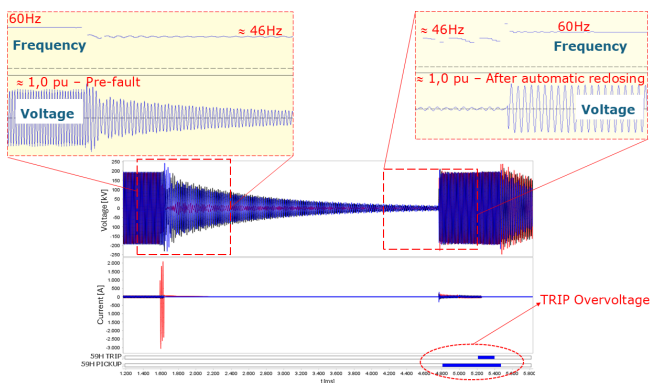

Figure 2: SE-A terminal disturbance oscillography

III. Laboratory Tests

In order to better understand the improper operation of the overvoltage function, it was decided to take the IED for laboratory testing, for fault injection. To perform the tests, it was decided to simulate the fault using the ATP/ATPDraw program [12], where the line parameters (LCC in ATP/ATPDraw) and the shunt reactor were modeled, to reproduce the frequency variation in the voltages during the dead time of automatic reclosing. This choice was necessary for the following reasons:

- The oscillography of the Digital Fault Recorder (DFR) of the Substation did not have the measurement of the 230 kV line voltage. Only the 230 kV busbar voltage.
- The IED oscillography has a sampling rate of 960 Hz (16 samples per cycle).
- The simulations were performed with a sampling rate of 5.0 kHz, that is, higher than that of the IED.

The waveforms obtained by the simulation are similar to the disturbance waveforms, which are initially suitable for testing.

A. Fault Injection through Test Suitcase

To validate the simulation, it was necessary to verify whether the IED would behave identically to the real case. Therefore, the waveform simulations were converted to the COMTRADE format of the joint standard IEC 60255-24 and IEEE C37.111 [13], which is compatible for application in test suitcases.

The IED was parameterized with the same settings as at the time of the disturbance and, when applying the simulated fault, the IED behaved in an identical manner to the disturbance, that is, the incorrect operation of the overvoltage protection was reproduced. By studying in detail the signals available in the IED's internal oscillography, it was verified that the calculated voltage phasor magnitudes, the measured frequency and the signal FT could be included in the equipment's parameterization. After inserting new parameterization into the IED with the aforementioned signals, the tests were repeated. Fig. 3 illustrates the results observed after including the new signals.
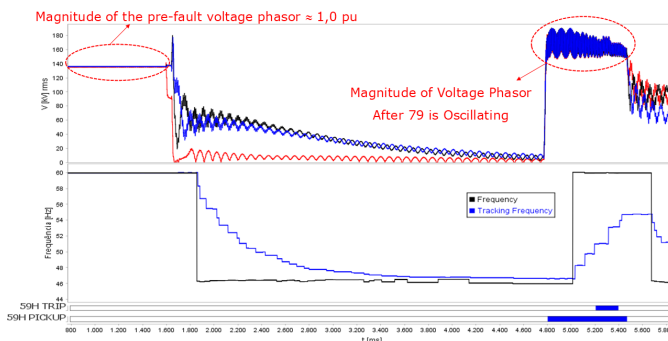

Figure 3: Voltage phasor magnitude, FT performed by the IED and actual measured frequency

It can be seen in Fig. 3 that the voltage magnitude were calculated incorrectly by the IED after the automatic reclosing, and that this error is due to the difference between the frequency of the voltage signals and the frequency tracked by the IED. These magnitude values were estimated with values higher than the real ones, causing the overvoltage function to operate incorrectly, which was adjusted to operate at 1.2 pu and with a timing of 400 ms. It is possible to see in Fig. 4 the values of the voltage magnitudes after the automatic reclosing, above the overvoltage function setting.

B. Evaluating IED Behavior for a Frequency Step

Through the simulated faults, it was possible to determine the behavior of the IED when subjected to a

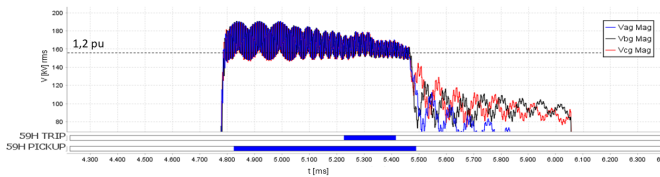frequency step from 46 to 60 Hz, as illustrated in Fig. 5.

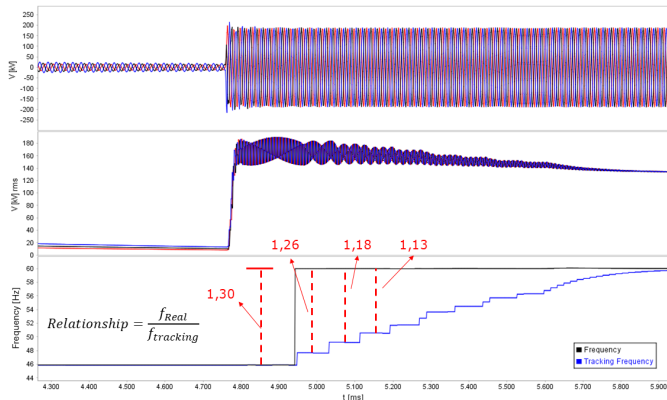Figure 4: Voltage magnitude value above overvoltage function setting

Figure 5: Behavior of the voltage magnitude, calculated by the IED, for a step in frequency

It was possible to verify that the calculated value of the voltage magnitude approaches its correct value when the value of the FT signal $f_{tracking}$ approaches the actual measured frequency f_{Real}, highlighting the almost zero error after 1.0 second from the beginning of the frequency step. It is noted that the FT signal, for the IED under analysis, began to change its value after 200 ms of the frequency step.

This result was only observed because the file resulting from the simulation was injected through the test suitcase, since in the real case the line circuit breaker opens after the overvoltage function operates.

After completing the laboratory testing stage, it was necessary to study the IED's internal algorithm in order to understand what actually caused the erroneous calculation of the voltage phasors and, in addition, to find a solution to the problem. Therefore, information was sought in the equipment manual, provided by the manufacturer, and in the literature in general, to identify similar situations.

IV. Frequency Tracking Algorithms

It is always desirable, for applications in the electrical system, that the frequency measurement is accurate and stable. However, the existing challenges

for developing frequency estimation algorithms must consider the dynamics of the measured signals [6].

The most widely used technique for determining frequency in protection relays is known as zero crossing [7] and, to improve accuracy, linear interpolation is used [4]. This method can be subject to spurious zero crossings, for this reason, pre-filtering with low-pass or band-pass filters can be used [14], however, it can affect the speed of frequency measurement [7]. It is possible to use currents, but voltages are preferred, because they are always larger in magnitude and are not affected by harmonics and DC decay, as much as by currents [7]. Generally, one of the voltage phases is chosen, such as: the voltage of phase A (VA). If this chosen signal is below a limit, the Clarke transform can be used to compose a new signal for tracking [4][7].

To ensure the correct functionality of the protection functions during frequency variations, IEDs have an internal mechanism called FT. This signal follows the measured frequency of a previously selected analog channel. In this way, the voltage and current phasor quantities are calculated for the actual system frequency and not for a previously defined nominal value, thus ensuring greater precision for the protection algorithms that may be required to operate in off-nominal frequency conditions during severe disturbances in the electrical system [6].

For application in phasor estimation, the FT mechanism must update its frequency measurement as quickly as possible in order to keep up with the system's frequency variations [6]. However, it is observed that the FT signal does not instantly follow the measured frequency; its value changes smoothly to ensure stability in phasor calculations. The FT signal is sent to the analog-to-digital converter, which uses this information to determine the time between samples in order to ensure a fixed number of samples per signal cycle.

In the disturbance under analysis, whose IED oscillography has a sampling rate of 960 Hz, that is, 16 samples per 60 Hz cycle, it can be seen in Fig. 6, which illustrates details of Fig. 2, that the change in time between samples is occurring as a function of the FT signal. The pre-fault moment can be seen (Fig. 6a), after the opening of the circuit breakers (Fig. 6b), the end of the dead time (Fig. 6c) and immediately after the automatic reclosing of the LT (Fig. 6d).

The actual frequency of the voltage signal and the value of the FT signal are recorded in Table I.

V. Phasor Estimation Algorithms

To better understand the behavior of high voltage in the disturbance, algorithms known in the literature
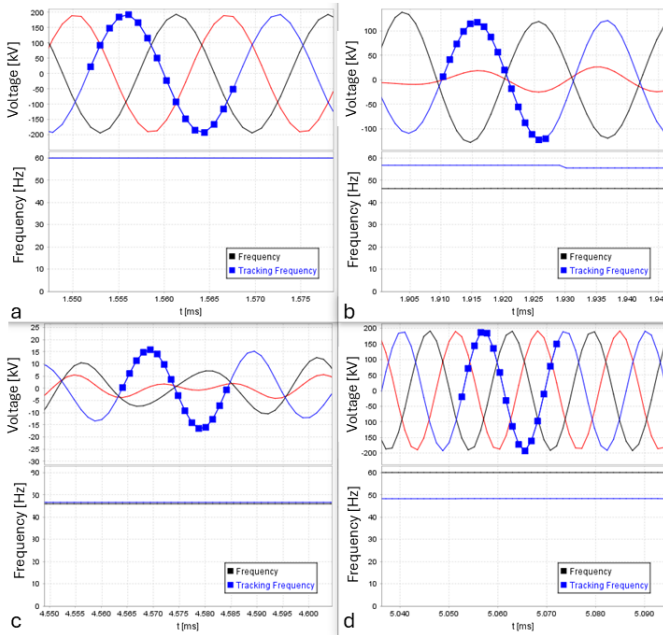
Figure 6: Sampling time variation following FT

Table I: Variation of frequency and FT during disturbance

	Measured Frequency	FT
Pre-fault	60.0 Hz	60.0 Hz
After opening the Circuit Breakers	46.8 Hz	60.0 Hz
End of dead time	46,7 Hz	46.9 Hz
Immediately after the line automatic reclosing	60.0 Hz	46.9 Hz

were researched. This article was based on evaluating the OCFF and HCFF [1], both based on the Discrete Fourier Transform (DFT) and the Least Squares Algorithm [2] for phasor estimation.

For this analysis, the influence of anti-aliasing filters was not considered, which are second-order low-pass analog filters present in the analog inputs of the IED, which are used before the analog-to-digital conversion to limit the frequency band and eliminate high-frequency noise [15].

A. One-Cycle and Half-Cycle Fourier Filters

Fourier-based phasor estimation algorithms began to be studied in the 1970s, due to the prospect of using computers for protection. The Fourier series has been considered a suitable technique for processing and sampling a waveform and determining its fundamental component [16]. The equations for calculating the real and imaginary parts of the phasor by means of the DFT for application in computers are presented in [1], that is, the beginning of digital relays.

The determination of phasors through the OCFF is performed through a sliding window of the size of one

cycle and uses the orthogonality of the cosine filters for the real part and sine filters for the imaginary part [17], whose equations are described in (1) and (2).

$$a_k = \frac{2}{N} \sum_{n=1}^{N} x_n cos\left(\frac{2\pi kn}{N}\right) \tag{1}$$

$$b_k = \frac{2}{N} \sum_{n=1}^{N} x_n sin\left(\frac{2\pi kn}{N}\right) \tag{2}$$

Where
$a_k \rightarrow$ Real part of the harmonic phasor k
$b_k \rightarrow$ Imaginary part of the harmonic phasor k
$x_n \rightarrow$ Sample n of the function to be analyzed
$N \rightarrow$ Number of samples in a cycle

Identical to OCFF, a sliding window is used for phasor estimation using a HCFF. However, the window size is half a period of a cycle of the periodic signal [18].

The real part a_k nd the imaginary part b_k of the phasors estimated by the application of HCFF are defined in (3) and (4).

$$a_k = \frac{4}{N} \sum_{n=1}^{\frac{N}{2}} x_n cos\left(\frac{2\pi kn}{N}\right) \tag{3}$$

$$b_k = \frac{4}{N} \sum_{n=1}^{\frac{N}{2}} x_n sin\left(\frac{2\pi kn}{N}\right) \tag{4}$$

The frequency response is illustrated, in Fig. 7a, to OCFF and, in Fig. 7b, to HCFF.
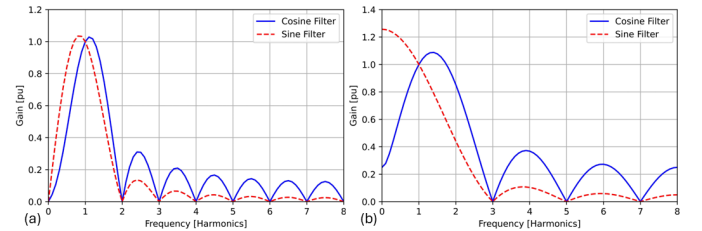

Figure 7: (a) OCFF and (b) HCFF frequency response for 960 Hz sampling rate

B. Least Squares Algorithm

The application of the least squares phasor estimation technique can be implemented with some variations. In this paper, four possible implementations will be shown, the difference between which is the inclusion or not of exponential decay, or the inclusion or not of even harmonics in the model that represents the waveform.

In the development of this technique, it was assumed that the anti-aliasing process will promote the elimination of harmonics higher than the fifth harmonic of voltage and current [2]. For this reason, the signal model

is expressed by exponential decay and harmonics up to the fifth order [2], as shown by (5).

$$y(t) = V_0 e^{\frac{t}{\tau}} + \sum_{k=1}^{K} V_k sin\left(k\omega_0 t + \theta_k\right) \tag{5}$$

Where

$y(t) \rightarrow$ Instantaneous value of the signal at time t

$\tau \rightarrow$ Time constant of the exponential decay

$\omega_0 \rightarrow$ Fundamental frequency of the system

$\theta_k \rightarrow$ Phasor angle of the kth harmonic

$V_0 \rightarrow$ Peak value of the exponential component

$K \rightarrow$ Order number of the largest harmonic present in the signal

After trigonometric manipulations, (5) is rewritten as follows, according to (6):

$$y(t) = V_0 e^{\frac{t}{\tau}} + \sum_{k=1}^{K} [V_k cos\left(\theta_k\right) sin\left(k\omega_0 t\right) + \\ V_k sin\left(\theta_k\right) cos\left(k\omega_0 t\right)] \tag{6}$$

The exponential decay term is expanded in the first terms of the Taylor series. For simplicity, only the first two terms were used, as per (7):

$$y(t) = V_0 - \frac{V_0}{\tau} t + \sum_{k=1}^{K} [V_k cos\left(\theta_k\right) sin\left(k\omega_0 t\right) + \\ V_k sin\left(\theta_k\right) cos\left(k\omega_0 t\right)] \tag{7}$$

The matrix equation is shown in (8):

$$[y] = [A][X] \tag{8}$$

Where

$[y] \rightarrow$ Matrix of measured sampled signals

$[A] \rightarrow$ Matrix of coefficients

$[X] \rightarrow$ Matrix of variables

The method is based on solving (8) in order to obtain the coefficients of matrix [X]. Matrix [A] is not square and the resolution of the equation involves finding the pseudo-inverse matrix of matrix [A], according to (9).

$$[A]^+ = \left[[A]^T [A]\right]^{-1} [A]^T \tag{9}$$

Where

$[A]^+ \rightarrow$ Pseudo-inverse matrix of the matrix [A]

The elements of the 3rd e 4th lines of $[A]^+$ are the filter coefficients to estimate the real and imaginary components of the fundamental frequency phasor of the signal.

1) Exponential decay included: For the signal model represented by (5), where the exponential decay component and harmonics up to the fifth order are considered, the frequency response of the filter applied for phasor estimation is illustrated in Fig. 8a. In this paper, this method is called LS1. According to [2], even harmonics are not observed in voltage and current signals

during faults. For this reason, the model, represented by (5), can be simplified, that is, even harmonics can be removed, and this method is called LS2, in this paper. The observed frequency response of the least-squares filter, when removing even harmonics, is shown in Fig. 8b.
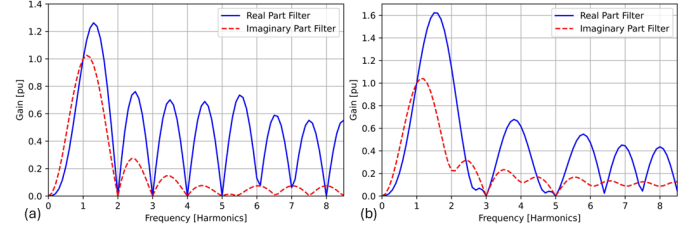

Figure 8: Least Squares frequency response with exponential decay and (a) even and odd harmonics included - LS1 - and, (b) only odd harmonics included - LS2 -, for 960 Hz sampling rate

In LS1, the frequency response of the filter dedicated to calculating the real part has gains greater than 1.2 for frequencies just above the fundamental frequency. In a slightly more expressive way, in LS2, the frequency response of the filter dedicated to calculating the real part has gains greater than 1.6 for frequencies just above the fundamental frequency. It can also be seen that frequencies close to even harmonics have gains with considerable values.

2) Harmonics only: The model of the signal to be estimated, the phasor, can be considered only sinusoidal, that is, without the expuential decay component, as per (10) and rewritten in (11), after trigonometric manipulations.

$$y(t) = \sum_{k=1}^{K} V_k sin\left(k\omega_0 t + \theta_k\right) \tag{10}$$

$$y(t) = \sum_{k=1}^{K} [V_k cos\left(\theta_k\right) sin\left(k\omega_0 t\right) + \\ V_k sin\left(\theta_k\right) cos\left(k\omega_0 t\right)] \tag{11}$$

The same technique is applied to obtain the pseudo-inverse matrix, i.e., the filter coefficients to estimate the real and imaginary parts.

The frequency response of the phasor estimation technique, using the least squares method, when considering the signal model without exponential decay, and only harmonics included, it called LS3, in this paper, is identical to the frequency response of the method using OCFF. It can be illustrated by Fig. 7, where the real part is represented by the cosine filter and the imaginary part is represented by the sine filter.

The observation that even harmonics can be disregarded, as reported in [2], was applied in the analysis of the least squares method for the signal model without the exponential decay portion, it called LS4, in this paper. The frequency response observed is also identical to the frequency response observed when the least squares technique is applied with even and odd harmonics.

VI. Comparison of Algorithms with the Real Case

Based on the analysis of the frequency response of the analyzed phasor estimation filters, it can be seen that, for most filters, the voltage magnitude will be below 1.2 pu (overvoltage sensor settings), when there is a signal with a frequency higher than the nominal frequency. The exceptions are for the real part filters of the least squares method, when the exponential component is considered.

When observing the frequency response of the real part of the least squares algorithm, it is observed that the value of the voltage magnitude obtained in the occurrence resembles the magnitude of a signal that could have used this filter. Considering that the IED is "tuned" to 46.9 Hz and the frequency of the voltage signal is 60 Hz, after reconnection, the relationship between the real frequency of the voltage signal and the FT is 1.28 pu and, according to the graph in Fig. 8a, a gain in the signal of 1.2 pu is observed. To illustrate this observation, Table II shows the gains as a function of frequency for the phasor estimation filters studied.

Table II: Filter gain for calculation of the real part of phasors

Frequency [pu]	Gain			
	OCFF/LS3/LS4	HCFF	LS1	LS2
0.6	0.5845	0.7225	0.3404	0.3164
0.7	0.7187	0.8067	0.4947	0.4614
0.8	0.8386	0.8818	0.6651	0.6293
0.9	0.9350	0.9466	0.8386	0.8121
1,0	1.0000	1.0000	1.0000	1.0000
1.1	1.0284	1.0412	1.1337	1.1814
1.2	1.0173	1.0697	1.2250	1.3447
1.3	**0.9669**	**1.0852**	**1.2621**	**1.4785**
1.4	0.8800	1.0877	1.2370	1.5731
1.5	0.7618	1.0774	1.1469	1.6213
1.6	0.6199	1.0546	0.9947	1.6188

Due to this similarity in behavior with the case studied, it is suspected that the combination of anti-aliasing filters, digital pre-filtering and the internal filter of the IED of this analysis, for voltage phasor estimation, has a frequency response close to the real part filter of the least squares considering the exponential decay. However, this information is not available from the manufacturer.

VII. Solution

The solution applied and tested in the laboratory consisted of changing the analog frequency reference channel to a voltage channel that is immune to oscillation resulting from the exchange of energy between the line capacitances and the shunt reactor at the SE-B terminal. This analog channel refers to the busbar Capacitive Potential Transformer and is used to perform the synchronization function, as seen in Fig. 1. This solution turned out to be simple, as it is only a change of internal parameters of the IED. Thus, whenever the line is opened by the circuit breakers, the frequency reference will be maintained by the bus voltage.

This analytical study was sent to the manufacturer, and as another solution, there was a recommendation/suggestion to change the frequency reference source when the circuit breaker opens, automatically, through changes in the IED's internal logic.

VIII. Conclusion

It was observed, through the analysis of the occurrence and the results obtained by the studies illustrated in this work, that when the estimation of the phasors is performed with a period window different from the period of a real signal cycle, there is the possibility of improper actuation of the protections, because the calculated value of the voltage magnitude by the IED is not consistent with the true value of the voltage measured on the line. This procedure adopted for the analysis of the occurrence was relevant, as it provided greater support for a better understanding of the actuation of the overvoltage protection relay and also in the training of human resources in the area of disturbance analysis at Eletrobras CGT Eletrosul.

References

[1] A. G. Phadke, T. Hlibka, and M. Ibrahim, "A digital computer system for ehv substations: Analysis and field tests," *IEEE Transactions on Power Apparatus and Systems*, vol. 95, no. 1, pp. 291–301, 1976.

[2] M. S. Sachdev and M. A. Baribeau, "A new algorithm for digital impedance relays," *IEEE Transactions on Power Apparatus and Systems*, vol. PAS-98, no. 6, pp. 2232–2240, 1979.

[3] E. O. Schweitzer and D. Hou, "Filtering for protective relays," in *IEEE WESCANEX 93 Communications, Computers and Power in the Modern Environment - Conference Proceedings*, 1993, pp. 15–23.

[4] D. Costello and K. Zimmerman, "Frequency tracking fundamentals, challenges, and solutions," in *2011 64th Annual Conference for Protective Relay Engineers*, 2011, pp. 203–214.

[5] M. M. Begovic, P. M. Djuric, S. Dunlap, and A. G. Phadke, "Frequency tracking in power networks in the presence of harmonics," *IEEE Transactions on Power Delivery*, vol. 8, no. 2, pp. 480–486, 1993.

[6] S. Xue, B. Kasztenny, I. Voloh, and D. Oyenuga, "Power system frequency measurement for frequency relaying," in *2007 Western Protective Relay Conference*, 10 2007.

[7] M. Ristic, I. Voloh, and Z. Zhang, "How frequency measurements can impact security of frequency elements in digital relays," in *2011 64th Annual Conference for Protective Relay Engineers*, 2011, pp. 366–384.

[8] SEL, *SEL-421-4,-5 Protection, Automation, and Control System – Instruction Manual*, Schweitzer Engineering Laboratories, 2021.

[9] GE, *D60 Line Distance Protection System – Instruction Manual*, GE Grid Solutions, 2023.

[10] SIEMENS, *Siprotec 5 Distance Protection, Line Differential Protection, and Overcurrent Protection for 3-pole Tripping 7SA82, 7SD82, 7SL82, 7SA86, 7SD86, 7SL86, 7SJ86 – Manual*, SIEMENS, 2024.

[11] HITACHI, *Line distance protection REL670 – Application manual*, HITACHI, 2024.

[12] F. P. H. K. Hoidalen, L. Prikler, *ATPDRAW: version 7.3 for Windows user's manual*, ATPDraw, 2021.

[13] IEEE/IEC, "Ieee/iec measuring relays and protection equipment – part 24: Common format for transient data exchange (comtrade) for power systems," *IEEE Std C37.111-2013 (IEC 60255-24 Edition 2.0 2013-04)*, pp. 1–73, 2013.

[14] M. S. Sachdev, R. Das, A. Apostolov, J. Holbach, T. Sidhu, J. Appleyard, B. Kasztenny, J. Soehren, K. Behrendt, T. Lanigan, G.Swift, O. Bolado, P. G. Mclaren, M. Thompson, G. Brunello, R. Patterson, D. Tziouvaras, J. Cornelison, and M. Saha, "Understanding microprocessor-based technology applied to relaying," Report of Working Group I16 of the Relaying Practices Subcommittee, Tech. Rep., 2004.

[15] P. V. B. Oliveira, R. L. A. Reis, D. Fernandes JR., and W. L. A. Neves, "Estimação de fasores de tensão em sistemas de transmissão: Uma abordagem sobre a influência do sistema de aquisição de dados," in *Sociedade Brasileira de Automática*, vol. 1, no. 1, 2019.

[16] P. G. McLaren and M. A. Redfern, "Fourier-series techniques applied to distance protection," *Proceedings on IEE*, vol. 122, no. 11, pp. 1301–1305, 1975.

[17] A. G. Phadke and J. S. Thorp, *Computer Relaying for Power System*. John Wiley & Sons Ltd, 2009.

[18] F. V. Lopes, D. Barros, C. Fernandes JR., J. Nascimento, N. Brito, W. Neves, and S. Moraes, "Influência de modelos de transformadores de potencial capacitivo sobre a estimação de fasores de tensão," in *Simpósio Brasileiro de Sistemas Elétricos*, 2012.